Table 1. Correlation among urinary PTCA, 6H5MI2C, 5-*S*-CD and 4-AHP

	Correlation coefficient [r^2 (P-values)]		
	Control subjects (n = 118)[a]	Melanoma patients (n = 45)	
Comparison	Normal scale	Normal scale	Log scale
PTCA versus 6H5MI2C	0.156 (n.s.)	0.142 (n.s.)	0.558 (<0.001)
PTCA versus 5-*S*-CD	0.001 (n.s.)	0.748 (<0.001)[b]	0.261 (<0.01)
PTCA versus 4-AHP	0.071 (n.s.)	0.041 (n.s.)	0.177 (n.s.)
6H5MI2C versus 5-*S*-CD	0.138 (n.s.)	0.094 (n.s.)	0.344 (<0.001)
6H5MI2C versus 4-AHP	0.118 (n.s.)	0.000 (n.s.)	0.155 (n.s.)
5-*S*-CD versus 4-AHP	0.005 (n.s.)	0.292 (<0.01)	0.634 (<0.001)

n.s., not significant.

[a]118 urine samples from 10 subjects collected over 1 yr period.

[b]A good correlation on normal scale was obtained because four samples with high values for PTCA and 5-*S*-CD lay closely on the same regression line.

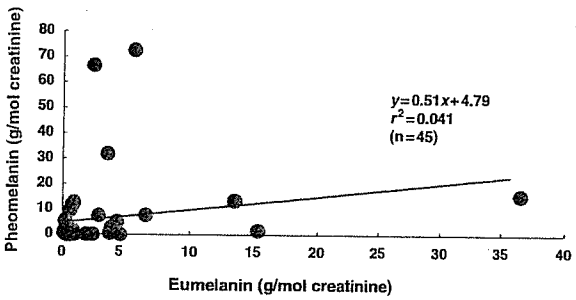

Figure 4. Relation between urinary levels of eumelanin and pheomelanin in 45 melanoma patients.

much pheomelanin compared with eumelanin. One patient excreted extremely high levels of eumelanin while two patients excreted even higher levels of pheomelanin.

Comparison of serum PTCA and 5-*S*-CD between control subjects and melanoma patients

It was found that serum PTCA could also be analysed with a similar method. A preliminary study was therefore carried out to evaluate the clinical significance of serum PTCA in melanoma. Serum levels of 5-*S*-CD in control subjects (n = 10) and melanoma patients (n = 10) used for this comparison were 4.0 ± 1.7 and 995 ± 957 nmol/l respectively. Serum levels of PTCA in those two groups were 40 ± 22 and 88 ± 73 nmol/l respectively. When compared in the median level, melanoma patients showed a 20-fold increase in serum 5-*S*-CD (73 versus 3.6) while the increase was only 2.0-fold in serum PTCA (69 versus 35).

Discussion

Clinical significance of serum or urinary 5-*S*-CD level in following the progression of melanoma has well been established in several studies (Agrup et al., 1979; Hartleb and Arndt, 2001; Horikoshi et al., 1994; Kärnell et al., 2000; Wakamatsu et al., 2002c). In contrast, serum or urinary 6H5MI2C level appears to be less sensitive than the corresponding 5-*S*-CD in detecting distant metastases (Horikoshi et al., 1994; Yamada et al., 1992). Also, serum pheomelanin (4-AHP) level is of less diagnostic value in melanoma diagnosis than serum 5-*S*-CD (Wakamatsu et al., 2003). Among other melanoma markers, S100B protein has been most thoroughly evaluated and acknowledged. A comparison study showed that among serum S100B and urinary 5-*S*-CD and 6H5MI2C, serum S100B protein was found to be the best prognostic marker, but urinary 5-*S*-CD was as nearly good as S100B (Kärnell et al., 1997). In the present study, we enrolled Japanese control subjects and Swedish melanoma patients. One would argue that there are large variations in urinary excretion of melanin-related metabolites among various ethnic origins differing in the degree of pigmentation. However, the differences between Japanese and Caucasians are expected to be approximately 2-fold for urinary levels of 6H5MI2C and much less for urinary 5-*S*-CD (Westerhof et al., 1987).

In the present study, we developed a HPLC method to quantify eumelanin (PTCA) in urine. Using this method, we have found that the urinary excretion of PTCA and 6H5MI2C in melanoma patients compared with control subjects is not so high as with 5-*S*-CD followed by 4-AHP. This indicates that urinary PTCA (and 6H5MI2C) is of little clinical value in following the progression of melanoma. On the contrary, urinary 4-AHP appears to be of considerable value in this respect.

The excretion of melanin in urine of melanoma patients is known as melanuria. Melanuria is, however, a rare finding in melanoma patients (Saghari et al., 2002). It is usually seen in patients with diffuse melanosis and primary or metastatic melanoma to the genitourinary tract. The present method to detect eumelanin in urine is highly sensitive as even urine samples with straw-yellow colour can give clear peaks of PTCA in HPLC chromatograms. However, the specific measurement

Pigment Cell Res. doi: 10.1111/j.1600-0749.2006.00296.x

of urinary eumelanin in the form of a degradation product PTCA did not appear to improve the clinical significance of 'melanuria'. On the contrary, the result shown in Figure 2 indicates that urinary pheomelanin (4-AHP) appears to be of considerable value in following melanoma progression. This appears to reflect the findings that (i) urinary 4-AHP levels in melanoma urine showed good correlation with urinary 5-*S*-CD levels (Takasaki et al., 2003) and (ii) in 60% of melanoma cases the excretion of pheomelanin is higher than the excretion of eumelanin.

At least two principal factors may influence the correlations between intermediate metabolites (e.g. 5-*S*-CD), endpoint metabolites (e.g. 6H5MI2C) and chemical degradation products of eumelanin (e.g. PTCA) and pheomelanin (e.g. 4-AHP). These factors are (i) the type of melanin (eumelanin, pheomelanin and mixture of these) and (ii) the production rate of melanin from the melanoma metastases and cell necrosis followed by excretion into the urine. Considering the first factor the high correlation between 6H5MI2C and PTCA can be expected from the fact that 6H5MI2C is an *O*-methylated derivative of DHICA, and PTCA is a degradation product of DHICA-derived melanin (Ito and Fujita, 1985). Similarly 5-*S*-CD is an intermediate product from the synthesis of pheomelanin and 4-AHP is a degradation product of pheomelanin. It might therefore be expected that these two compounds should be correlated. Considering the second factor, there might also be a correlation between the intermediate product 5-*S*-CD (released from the cytoplasm of the pigment cell) and PTCA in particular if the production of eumelanin is high in the melanosome. A high correlation on linear scale was obtained mainly because of three samples with extremely high values for PTCA and 5-*S*-CD lay closely on the same regression line which would indicate a high production of melanin. As their urinary pigment may be of different character – eumelanin, pheomelanin and mixtures of these – we think that such urinary pigment, being water soluble, would be an interesting material for further characterization of human melanin structure. In this connection, it should be pointed out that a majority (60%) of melanoma cases excreted pheomelanin-rich pigment. Pheomelanin is rather water soluble under neutral to alkaline conditions (Ozeki et al., 1995).

Serum levels of PTCA were also examined in control subjects and melanoma patients. The result shows that serum PTCA levels do not increase even in patients with very high levels of serum 5-*S*-CD, indicating that serum PTCA is not useful in following the progression of melanoma.

Finally, it is well known that levels of urinary and serum (plasma) 5-*S*-CD show seasonal variation with higher values in summer and lower values in winter (Nimmo et al., 1988; Rorsman et al., 1976; Wakamatsu and Ito, 1995). Interestingly, urinary PTCA levels also show seasonal variation (Figure 3). However, the large fluctuation in each control subjects makes the urinary PTCA of little value as a marker for the degree of pigmentation. Seasonal variation is also seen in levels of urinary and serum 6H5MI2C in our ongoing study (unpublished results).

Materials and methods

Subjects

Control urine samples were obtained from 10 control Japanese subjects aged 25–59 yr (38 ± 15). Their one-time urine samples were collected randomly in the middle of every month starting from October 2003 to September 2004. Approximately 7 ml of urine was taken to plastic tubes containing 200 μl of acetic acid. A total of 120 urine samples were used for this study, but two samples were excluded because serum samples taken on the same occasions gave abnormally 5-*S*-CD high values. Melanoma urine samples were obtained from 45 Swedish patients with various degrees of progression. The 45 samples correspond to the 51 samples described in Takasaki et al. (2003). These urine samples were stored frozen at −70°C until analysis. 6H5MI2C and 5-*S*-CD in urine are rather stable under these conditions (Kågedal et al., 1992). Determinations of urinary 5-*S*-CD and 4-AHP in Swedish melanoma patients were carried out in Sweden (Takasaki et al., 2003).

Control serum samples were obtained from the same 10 Japanese subjects as for the urine samples in September 2004. Serum samples from melanoma patients were obtained from 10 Japanese patients at stage IV who had serum 5-*S*-CD levels exceeding 100 nmol/l. Cut-off value of serum 5-*S*-CD is 10 nmol/l (Wakamatsu et al., 1991, 2002c).

Determination of urinary levels of 6H5MI2C, 5-*S*-CD, and pheomelanin (4-AHP)

Determination of urinary 6H5MI2C was performed using HPLC, mostly as previously described (Wakamatsu et al., 1991). A modification was to use a fluorescent detector, JASCO FP-2020 (JASCO Co., Tokyo, Japan), instead of the originally described electrochemical detector. The excitation wavelength was 315 nm and the emission wavelength 390 nm. Determination of urinary 5-*S*-CD was performed using HPLC with electrochemical detection, as previously reported (Kågedal et al., 1989; Wakamatsu and Ito, 1994). Determination of urinary 4-AHP was performed using HPLC with electrochemical detection as previously reported (Takasaki et al., 2003; Wakamatsu et al., 2003). Levels of analytes were calculated against creatinine as described by Kärnell et al. (2000).

Determination of urinary levels of eumelanin (PTCA)

For analysis of urinary PTCA, 200 μl urine was mixed with 700 μl 0.1 M H_2SO_4 and 100 μl homogenate of mouse livers (Ito and Fujita, 1985; Ito and Wakamatsu, 1994). To the mixture was added 3% $KMnO_4$ in 20-μl portions under vigorous mixing. Ten minutes later, excess $KMnO_4$ was decomposed with 100 μl 10% Na_2SO_3. The colourless mixture was extracted with two portions of approximately 7 ml ether. The combined ether extract was evaporated with aspirator, and the residue was dissolved in 200 μl water. Forty microlitre of the solution was injected into the HPLC system as described below. Serum PTCA was determined with 100 μl serum.

Pyrrole-2,3,5-tricarboxylic acid was analysed with an HPLC system consisting of a JASCO 980-PU liquid chromatograph, a Shiseido C18 column (Capcell pak C18; 4.6 × 250 mm; 5 μm particle size), and a JASCO 875-UV detector. The mobile phase used was 0.1 M potassium phosphate buffer, pH 2.10:methanol, 99:1 (vol/vol). The analyses were performed at 50°C at a flow rate of

0.7 ml/min. The UV detector was set at 269 nm. We usually injected 91 ng of PTCA as a standard.

A possibility that PTCA might be derived from 6H5MI2C was examined by oxidizing 6H5MI2C with permanganate. The yield was 5.0 μg PTCA from 1 mg 6H5MI2C. It is therefore confirmed that unless 6H5MI2C is present at extremely high levels, the contribution of 6H5MI2C to PTCA value is negligible. Likewise, the contribution of 5-*S*-CD and pheomelanin are also negligible (Ito and Fujita, 1985), based on the yields of PTCA: 0.09 and 0.17 μg/mg from 5-*S*-CD and pheomelanin respectively. The recovery of PTCA was examined by oxidizing with permanganate a pooled urine sample added with a 20 μg/ml final concentration of *Sepia* melanin (from Sigma Chemical Company, Toyko, Japan).

The peak fraction with the same retention time as PTCA in HPLC was collected from a control urine sample and the eluates were pooled and evaporated in a desiccator and subjected to the LC/MS/MS analysis using an electronspray ionization/ion trap mass spectrometer (LCQ Deca XP, Thermoelectron, Tokyo, Japan). The analysis was carried out directly by the MS/MS at negative charge.

Statistical analysis

Differences were analysed for statistical significance using the Mann–Whitney *U*-test. P-values <0.05 are considered to be significant. Pearson correlation coefficients were calculated to measure the association between PTCA, 6H5MI2C, 5-*S*-CD and 4-AHP.

Acknowledgements

This study was supported in part, by a Grant-in-Aid for Cancer Research (15–10) from the Ministry of Health, Labour, and Welfare of Japan and in part by grants from the Swedish Cancer Society (Project 2357-B01-16XAA), from The Health Research Council in the Southeast of Sweden, and from the University Hospital, Linköping.

References

Agrup, G., Agrup, P., Andersson, T., Hafström, L., Hansson, C., Jacobsson, S., Jönsson, P.-E., Rorsman, H., Rosengren, A.-M., and Rosengren, E. (1979). 5 years' experience of 5-*S*-cysteinyldopa in melanoma diagnosis. Acta Derm. Venerol. *59*, 381–388.

Ekelund, M.C., Carstam, R., Hansson, C., Rorsman, H., and Rosengren, E. (1985). Urinary excretion of 5-*S*-cysteinyldopa and 6-hydroxy-5-methoxyindole-2-carboxylic acid: differences between pigmented and albino mice. Acta Derm. Venereol. *65*, 437–439.

Hartleb, J., and Arndt, R. (2001). Review. Cysteine and indole derivatives as markers for malignant melanoma. J. Chromatogr. B. *764*, 409–443.

Hearing, V.J. (1998). The regulation of melanin production. In The Pigmentary System. Physiology and Pathophysiology, J.J. Nordlund, R. Boissy, V.J. Hearing, R.A. King, and J.-P. Ortonne eds. (New York: Oxford University Press), pp. 423–438.

Horikoshi, T., Ito, S., Wakamatsu, K., Onodera, H., and Eguchi, H. (1994). Evaluation of melanin-related metabolites as markers of melanoma progression. Cancer *73*, 629–636.

Ito, S. (2003). A chemist's view of melanogenesis. Pigment Cell Res. *16*, 230–236.

Ito, S., and Fujita, K. (1985). Microanalysis of eumelanin and pheomelanin in hair and melanomas by chemical degradation and liquid chromatography. Anal. Biochem. *144*, 523–536.

Ito, S., and Wakamatsu, K. (1994). An improved modification of permanganate oxidation of eumelanin that gives a constant yield of pyrrole-2,3,5-tricarboxylic acid. Pigment Cell Res. *7*, 141–144.

Kågedal, B., Källberg, M., Årstrand, K., and Hansson, C. (1989). Automated high-performance liquid chromatographic determination of 5-*S*-cysteinyl-3,4-dihydroxyphenylalanine in urine. J. Chromatogr. *473*, 359–370.

Kågedal, B., Lenner, L., Årstrand, K., and Hansson, C. (1992). The stability of 5-*S*-cysteinyldopa and 6-hydroxy-5-methoxyindole-2-carboxylic acid in human urine. Pigment Cell Res. *5* (Suppl. 2), 304–307.

Kärnell, R., von Schoultz, E., Hansson, L.,O., Nilsson, B., Årstrand, K., and Kågedal, B. (1997). S100B protein, 5-*S*-cysteinyldopa and 6-hydroxy-5-methoxyindole-2-carboxylic acid as biochemical markers for survival prognosis in patients with malignant melanoma. Melanoma. Res. *7*, 393–399.

Kärnell, R., Kågedal, B., Lindholm, C., Nilsson, B., Årstrand, K., and Ringborg, U. (2000). The value of cysteinyldopa in the follow-up of disseminated malignant melanoma. Melanoma. Res. *10*, 363–369.

Liu, Y., Hong, L, Kempf, V.R., Wakamatsu, K., Ito, S., and Simon, J.D. (2004). Ion-exchange and adsorption of Fe(III) by *Sepia* melanin. Pigment Cell Res. *17*, 262–269.

Nimmo, J.E., Gawkrodger, D.J., O'Docherty, C.S.J., Going, I.W., Percy-Robb, I.W., and Hunter, J.A.A. (1988). Plasma 5-*S*-cysteinyldopa as an index of melanogenesis. Br. J. Dermatol. *118*, 487–496.

Ozeki, H., Ito, S., Wakamatsu, K, and Hirobe, T. (1995). Chemical characterization of hair melanins in various coat-color mutants of mice. J. Invest. Dermatol. *105*, 361–366.

Ozeki, H., Ito, S., Wakamatsu, K, and Thody, A.J. (1996). Spectrophotometric characterization of eumelanin and pheomelanin in hair. Pigment Cell Res. *9*, 265–270.

Rorsman, H., Agrup, G., Falck, B., Rosengren, A.M., and Rosengren, E. (1976). Exposure to sunlight and urinary excretion of 5-*S*-cysteinyldopa. In Pigment Cell, vol 2, V. Riley, ed. (Baesl: Karger), pp. 284–289.

Saghari, S., Bakshandeh, H., and Kerdel, F. (2002). Sudden onset of melanuria in patient with metastatic melanoma and toxic epidermal necrolysis. Int. J. Dermatol. *41*, 116–118.

Takasaki, A., Nezirevic, D., Årstrand, K., Wakamatsu, K., Ito, S., and Kågedal, B. (2003). HPLC analysis of pheomelanin degradation products in human urine. Pigment Cell Res. *16*, 480–486.

Wakamatsu, K., and Ito, S. (1994). Improved HPLC determination of 5-*S*-cysteinyldopa in serum. Clin. Chem. *40*, 495–496.

Wakamatsu, K., and Ito, S. (1995). Seasonal variation in serum concentration of 5-*S*-cysteinyldopa and 6-hydroxy-5-methoxyindole-2-carboxylic acid in healthy Japanese. Pigment Cell Res. *8*, 132–134.

Wakamatsu, K., and Ito, S. (2002a). Advanced chemical methods in melanin determination. Pigment Cell Res. *15*, 174–183.

Wakamatsu, K., Ito, S., and Fujita, K. (1990). Production, circulation, and excretion of melanin-related metabolites in B16 melanoma-bearing mice. Acta Derm. Venereol. *70*, 367–372.

Wakamatsu, K., Ito, S., and Horikoshi, T. (1991). Normal values of urinary excretion and serum concentration of 5-*S*-cysteinyldopa and 6-hydroxy-5-methoxyindole-2-carboxylic acid, biochemical markers of melanoma progression. Melanoma. Res. *1*, 141–147.

Wakamatsu, K., Ito, S., and Rees, J.L. (2002b). The usefulness of 4-amino-3-hydroxyphenylalanine as a specific marker of pheomelanin. Pigment Cell Res. *15*, 225–232.

Wakamatsu, K., Kageshita, T., Furue, M., Hatta, N., Kiyohara, Y., Nakayama, J., Ono, T., Saida, T., Takata, M., Tsuchida, T. et al. (2002c). Evaluation of 5-*S*-cysteinyldopa as a marker of melanoma progression: 10 years' experience. Melanoma. Res. *12*, 245–253.

Wakamatsu, K., Yokochi, M., Naito, A., Kageshita, T., and Ito, S. (2003). Comparison of phaeomelanin and its precursor 5-*S*-cysteinyldopa in the serum of melanoma patients. Melanoma. Res. *13*, 357–363.

Westerhof, W., Pavel, S., Kammeyer, A., Beusenberg, F.D., and Cormane, R. (1987). Melanin-related metabolites as markers of the skin pigmentary system. J. Invest. Dermatol. *95*, 78–81.

Wirestrand, L.E., Hansson, C., Rosengren, E., and Rorsman, H. (1985). Melanocyte metabolites in the urine of people of different skin colour. Acta Derm. Venereol. (Stockh.) *65*, 435–437.

Yamada, K., Walsh, N., Hara, H., Jimbow, K., Chen, H., and Ito, S. (1992). Measurement of eumelanin precursor metabolites in the urine as a new marker for melanoma metastases. Arch Dermatol. *128*, 491–494.

Short Communication
doi: 10.1111/j.1600-0749.2006.00324.x

Evaluation of melanin-related metabolites as markers of solar ultraviolet-B radiation

Kazumasa Wakamatsu* and Shosuke Ito

Department of Chemistry, Fujita Health University School of Health Sciences, Toyoake, Aichi 470-1192, Japan
*Address correspondence to Kazumasa Wakamatsu,
e-mail: kwaka@fujita-hu.ac.jp

Summary

Ultraviolet-B (UVB) radiation due sunlight can result in sunburns and/or suntans. Sunburn occurs only several hours after solar UVB radiation, while a suntan requires several days to several weeks to develop. In the present study, we measured serum and urine levels of melanin-related metabolites, 5-*S*-cysteinyldopa (5-*S*-CD) and 6-hydroxy-5-methoxyindole-2-carboxylic acid (6H5MI2C), in nine subjects exposed to normal sunlight over the course of 12 months. We collected samples in the middle of each month and examined the variation of the markers, the correlation between them, and their correlation with solar UVB radiation. Those markers exhibited a seasonal variation with lower values in the winter and higher values in the summer. Levels of 5-*S*-CD and 6H5MI2C in the serum showed 48% and 54% increases in the summer compared with those in the winter, respectively. Comparison of 5-*S*-CD in the serum and urine showed the highest correlation (r^2 = 0.344), followed by the pair of 5-*S*-CD and 6H5MI2C in the serum. Levels of 5-*S*-CD in the serum showed the highest correlation (r^2 = 0.729) with the mean solar UVB radiation during the first 10 d of the month, while 6H5MI2C in the serum was highly correlated (r^2 = 0.483) with solar UVB radiation during the previous month. Levels of 5-*S*-CD and 6H5MI2C in the serum appear to reflect the degrees of skin injury and pigmentation in the skin, respectively.

Key words: 5-*S*-Cysteinyldopa/eumelanin/6-hydroxy-5-methoxyindole-2-carboxylic acid/sunlight/ultraviolet radiation

Received 20 October 2005, revised and accepted 15 May 2006

Introduction

Sunlight is composed of three main regions of wavelengths: ultraviolet (UV), visible and infrared. UV radiation is further divided into three sections: ultraviolet-A (UVA) (320–400 nm), ultraviolet-B (UVB) (280–320 nm) and ultraviolet-C (UVC) (200–280 nm). UVC is effectively blocked from reaching the earth's surface by the ozone layer. While UVA is supposed to cause ageing and wrinkling of the skin, UVB is considered to play the major role in acute effects of UV radiation. The acute effects of UVB radiation comprise sunburn (erythema) and suntan (enhanced melanin production) (Matsumura and Anathaswamy, 2004). Sunburn is the most conspicuous acute response to UVB radiation, particularly in light-skinned individuals. This occurs within several hours after excessive UVB radiation. Suntan occurs several days to several weeks after UVB radiation by activating melanocytes to increase melanin production. Repeated UVB radiation increases the number of melanocytes, which may also contribute to the increased production of melanin (Stierner, 1991).

Melanocytes produce melanins and melanin-related metabolites, most of which are retained in the melanocytes, but some are secreted into the blood and then excreted into the urine. It is thus expected that the levels of these melanin-related compounds in the serum or urine may reflect the degree of pigmentation (Hansson, 1988; Stierner, 1991). The production of melanin pigment is catalysed by the specific enzyme tyrosinase, which converts L-tyrosine to dopaquinone (Hearing, 1998; Ito, 2003). Dopaquinone is a highly reactive molecule, and is rapidly cyclized to form dopachrome which is then either decarboxylated to give 5,6-dihydroxyindole (DHI) or tautomerized to give 5,6-dihydroxyindole-2-carboxylic acid (DHICA). DHI and DHICA are then oxidized to form eumelanin, a dark brown to black pigment. However, a significant portion of DHICA leaks into the blood stream and is excreted in the urine after *O*-methylation to 6-hydroxy-5-methoxyindole-2-carboxylic acid (6H5MI2C) or its isomer 5H6MI2C (Wakamatsu et al., 1990; Westerhof et al., 1987). These indolic eumelanin metabolites are thus considered to reflect tyrosinase activity in melanocytes (Ekelund et al., 1985; Wakamatsu et al., 1990; Westerhof et al., 1987).

However, in the presence of cysteine, dopaquinone binds to that to form 5-*S*-cysteinyldopa (5-*S*-CD) along with minor isomers (Ito, 2003). The oxidation of cysteinyldopa isomers in melanocytes leads to the production of pheomelanin, a yellow to reddish melanin, but a significant portion of cysteinyldopas escapes from melanocytes (Wakamatsu et al., 1990). Therefore, levels of 5-*S*-CD in the serum or urine have been used to estimate the progression of melanoma (Agrup et al., 1979; Kärnell et al., 2000; Wakamatsu et al., 2002).

Ultraviolet-B radiation is known to increase the level of 5-*S*-CD in the serum (Hansson et al., 1981; Nimmo et al., 1988; Tegner et al., 1983) or in the urine (Agrup et al., 1978; Stierner, 1991; Stierner et al., 1988). The UVB-induced increase of 5-*S*-CD is thought to be due to melanocyte injury (sunburn). On the contrary, the eumelanin-related metabolites, 6H5MI2C and 5H6MI2C, are considered good markers for the production of melanin pigment in the skin (Ekelund et al., 1985; Hansson, 1988; Westerhof et al., 1987).

In the present study, we measured levels of 5-*S*-CD and 6H5MI2C in the serum and urine of nine subjects over the course of 12 months to examine their monthly variation, the correlation between them and their correlation with solar UVB radiation. Serum levels of 5-*S*-CD and 6H5MI2C were found to reflect the degree of solar UVB radiation in the immediate past and in the previous month, respectively.

Results

Monthly variation of levels of melanin-related metabolites in the serum and urine

Nine normal subjects were analyzed every month for levels of melanin-related metabolites, 5-*S*-CD and 6H5MI2C in their serum and urine. Figure 1 shows the monthly variation in the mean values of the markers. All of the markers exhibited seasonal variation, with lower values in the winter and higher values in the summer.

To more precisely evaluate the increases in the summer, we compared the mean levels in the winter (December to February) with those in the summer (June to August). As shown in Table 1, all markers showed significant increases in the summer. Serum 5-*S*-CD levels showed a 48% increase ($P < 0.001$), while serum and urinary levels of 6H5MI2C showed 54% ($P < 0.001$) and 122% ($P < 0.001$) increases, respectively.

Correlation between solar UVB radiation and levels of melanin-related metabolites in the serum and urine

The correlation coefficients among the markers are summarized in Table 2. The pair of serum and urinary 5-*S*-CD levels showed the highest correlation ($r^2 = 0.344$), followed by the pair of serum 5-*S*-CD and serum 6H5MI2C ($r^2 = 0.246$). On the other hand, the pair of serum and urinary 6H5MI2C did not show a high correlation ($r^2 = 0.156$).

The correlation coefficients between solar UVB radiation and the markers are summarized in Table 3. Levels of serum 5-*S*-CD showed the highest correlation with the mean daily solar radiation during the first 10 d of the month ($r^2 = 0.729$; Figure 2A), followed by urinary 6H5MI2C ($r^2 = 0.462$).

When a comparison was made with solar UVB radiation during the previous month, the levels of serum 6H5MI2C showed a better correlation ($r^2 = 0.483$; Figure 2B). The other markers had similar or poorer correlations. The regression curves showed the presence of basal levels independent of UVB radiation (when $x = 0$).

Discussion

Melanin-related metabolites, especially 5-*S*-CD and 6H5MI2C, have been extensively evaluated as markers of pigmentation (Hansson, 1988; Nimmo et al., 1988; Stierner, 1991; Westerhof et al., 1987). From those studies, it appears that the levels of 5-*S*-CD in the

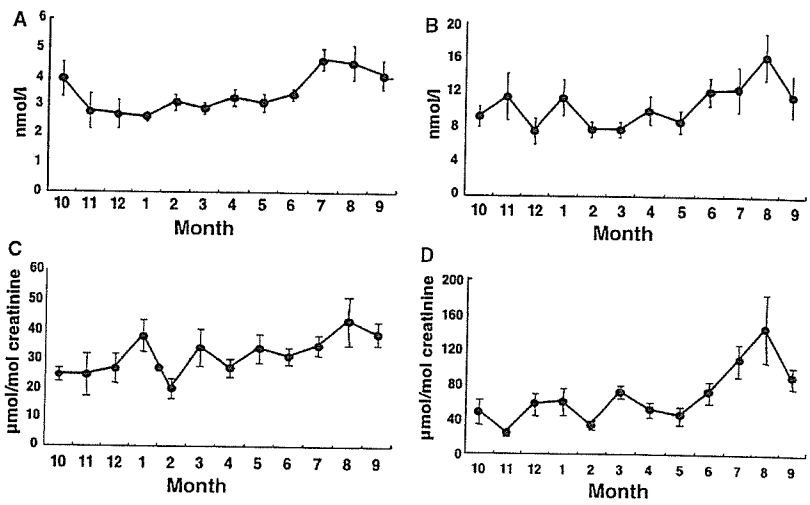

Figure 1. Monthly variation of levels of melanin-related metabolites. (A) serum 5-*S*-CD; (B) serum 6H5MI2C; (C) urinary 5-*S*-CD; (D) urinary 6H5MI2C. Mean ± SE ($n = 9$).

Table 1. Comparison of levels of melanin-related metabolites between winter and summer seasons[a]

Marker (nmol/l for serum or μmol/mol creatinine for urine)	Winter[a]	Summer[a]	S/W ratio[b]	P-value
Serum 5-*S*-CD	2.82 ± 0.21	4.18 ± 0.26	1.48	<0.001
Serum 6H5MI2C	8.81 ± 0.92	13.6 ± 1.37	1.54	<0.001
Urinary 5-*S*-CD	27.5 ± 2.92	36.0 ± 3.19	1.31	<0.05
Urinary 6H5MI2C	48.5 ± 6.85	108 ± 15.5	2.22	<0.001

[a]Winter values were obtained as averages for December, January and February, while summer values were for June, July and August. Averages for nine subjects were compared between winter and summer seasons. Mean ± SE.
[b]Average ratio of summer to winter values.

Table 2. Correlation of levels of melanin-related metabolites among each marker[a]

Pair of markers	r^2 value	P-value
Serum 5-*S*-CD versus urinary 5-*S*-CD	0.344	<0.001
Serum 6H5MI2C versus urinary 6H5MI2C	0.156	<0.001
Serum 5-*S*-CD versus serum 6H5MI2C	0.246	<0.001
Urinary 5-*S*-CD versus urinary 6H5MI2C	0.193	<0.001
Serum 5-*S*-CD versus urinary 6H5MI2C	0.191	<0.001
Serum 6H5MI2C versus urinary 5-*S*-CD	0.107	<0.001

[a]Values are correlation coefficients (r^2) for the 106 serum or urine samples from nine subjects.

serum or urine do not reflect melanin production but rather correspond to skin injury due to UVB radiation. On the contrary, 6H5MI2C, a eumelanin-related metabolite, is considered as the best marker of melanin production (Ekelund et al., 1985; Westerhof et al., 1987; Wirestrand et al., 1985).

In the present study, we examined the monthly variation in levels of 5-*S*-CD and 6H5MI2C in the serum and urine of nine subjects. This is the first comprehensive study to compare those metabolites as markers of solar UVB radiation. Among those markers, the levels of 5-*S*-CD in the serum and urine showed the best correlation for individual values. On the other hand, the levels of 6H5MI2C in the serum and urine showed a rather poor correlation. This may be ascribed to the excretion of some 6H5MI2C as conjugates with sulfuric acid or glucuronic acid (Wakamatsu and Ito, 1990). In previous studies, no correlation was found in basal levels of 5-*S*-CD or 6H5MI2C in the urine of Caucasian adults (Wirestrand et al., 1985) or children (Meyerhöffer et al., 1998). Furthermore, levels of 5-*S*-CD and 6H5MI2C in the serum showed only a negligible correlation (r^2 = 0.078; Wakamatsu and Ito, 1995). Westerhof et al. (1987) claimed that 5H6MI2C is the best urinary marker of melanin production. We found, however, that both in the serum and urine, levels of 5H6MI2C were much lower than those of 6H5MI2C (data not shown) and measurements of 5H6MI2C were more difficult due to interfering peaks. Moreover, measurement of the 6H5MI2C conjugates in the urine was not performed because we expected difficulty in HPLC separation of those compounds (Wakamatsu and Ito, 1990).

The levels of 5-*S*-CD and 6H5MI2C showed seasonal variations, with high values in the summer and low values in the winter. The most significant increases in the summer were noted in the levels of 5-*S*-CD in the serum and in the levels of 6H5MI2C in the urine. Seasonal variation in the levels of melanin-related metabolites has been examined in several studies. The excretion of 5-*S*-CD in the urine was found to increase threefold in the summer (Rorsman et al., 1976). Nimmo et al. (1988) then showed that levels of 5-*S*-CD in the plasma were low in the winter season and were high in the early summer in Edinburgh, UK. We have also found a similar seasonal variation of levels of 5-*S*-CD in the serum of Japanese (Wakamatsu and Ito, 1995).

In this study, among the markers examined, levels of 5-*S*-CD in the serum (taken in the middle of each month) were found to reflect best the solar UVB radiation in the immediate past (the first 10 d of the month). In a previous study, we reported a similar,

Table 3. Correlation of levels of melanin-related metabolites to solar UVB radiation during the first 10 d or the previous month

	With the first 10 d of the month		With the previous month	
Marker	Linear regression[a]	Correlation[b]	Linear regression[a]	Correlation[b]
Serum 5-*S*-CD	$y = 0.071x + 2.35$	0.729	$y = 0.066x + 2.45$	0.560
Serum 6H5MI2C	$y = 0.207x + 7.40$	0.353	$y = 0.224x + 7.15$	0.483
Urinary 5-*S*-CD	$y = 0.434x + 24.5$	0.278	$y = 0.467x + 24.2$	0.286
Urinary 6H5MI2C	$y = 3.02x + 20.6$	0.462	$y = 2.87x + 24.4$	0.420

[a]*x*-axis represents the mean value of daily solar UVB radiation for each month (mJ/cm^2); *y*-axis represents the mean value (n = 9) of each marker for each month.
[b]Correlation coefficient (r^2).

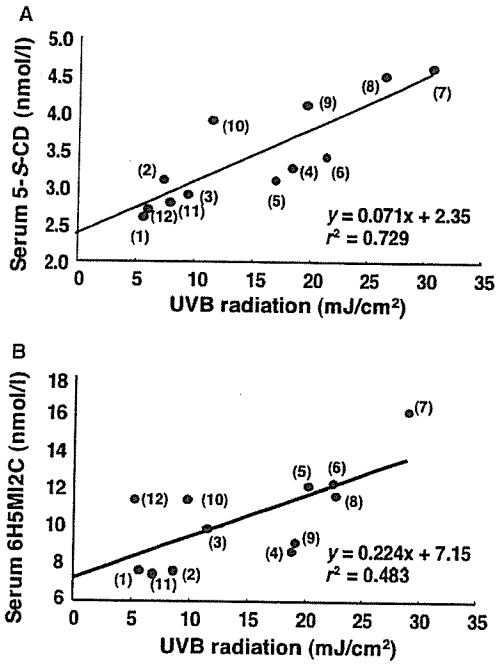

Figure 2. Correlation of levels of melanin-related metabolites to solar UVB radiation. Blood collection was done in the middle (13–17 d) of each month. Parenthesis indicates the month of collection. (A) Serum 5-*S*-CD levels versus solar UVB radiation in the first 10 d of the month, indicating that the impact of the UVB radiation could be seen within days. (B) Serum 6H5MI2C levels versus solar UVB radiation in the previous month, indicating that the impact of the UVB radiation could be seen within weeks.

moderate correlation of levels of 5-*S*-CD in the serum with solar radiation over 24 months ($r^2 = 0.230$) (Wakamatsu and Ito, 1995). Stierner et al. (1988) showed that during UVB radiation, subjects with skin type II had a significantly higher excretion of 5-*S*-CD than did those with skin types III–IV. Levels of 5-*S*-CD in the serum were found to increase markedly 3 d after UVA radiation, although no increase in pigmentation was noted (Hansson et al., 1981; Tegner et al., 1983). These findings, coupled with the results of other studies (Nimmo et al., 1988; Stierner, 1991), strongly suggest that the UVB-induced increase in levels of 5-*S*-CD in the serum and urine is not due to an increased synthesis of melanin, but instead reflects UVB-induced skin injury (sunburn). The present study shows that levels of 5-*S*-CD in the serum respond within 5–15 d to solar UVB radiation. This further supports the concept that 5-*S*-CD is a good marker of sunburn in the skin.

In contrast to levels of 5-*S*-CD in the serum, levels of 6H5MI2C in the serum were found to reflect well UV radiation in the previous month, indicating the delayed response to UV radiation (suntan). This fits well with previous findings that levels of 6H5MI2C in the urine are higher in individuals with dark skin than in those with fair skin (Westerhof et al., 1987; Wirestrand et al., 1985) and that 6H5MI2C is not found in the urine of albino mice (Ekelund et al., 1985). We, therefore, propose that levels of 6H5MI2C in the serum be used as a marker of pigmentation (suntan) after solar UV radiation.

In this study, urinary levels of 5-*S*-CD and 6H5MI2C were more variable and less informative than serum levels. This could be partly due to the method of collection; 24-h urine collection would have led to more consistent results.

The presence of basal levels of 5-*S*-CD and 6H5MI2C may be explained by UVB-independent production of those melanin-related metabolites. Tyrosine residues in proteins are oxidized by oxygen radicals to form protein-bound dopa (Rodgers and Dean, 2000). Free dopa, released from protein-bound dopa, could serve as a precursor for the basal levels of 5-*S*-CD and 6H5MI2C.

In conclusion, levels of 5-*S*-CD and 6H5MI2C in the serum appear to reflect the degree of injury (sunburn) and pigmentation (suntan) in the skin, respectively.

Materials and methods

Subjects

Serum and urine samples were obtained from nine normal Japanese subjects (four males and five females), aged 22–59 yr (35.8 ± 14.5 yr old) in the middle (13–17 d) of every month, starting from October 2003 to September 2004. None of the subjects intentionally avoided exposure to sunlight. However, as either students or professionals at our University, they did not usually perform daily outside activities during weekdays. Two of the four males spent several hours outside for hiking or baseball irregularly during weekends. Blood samples were drawn by venipuncture into vacuum tubes in the absence of heparin and were allowed to coagulate. Sera were separated by centrifugation and stored at −70°C until analysis. Urine samples were collected randomly on the same day as the serum collection. Approximately 7 ml of urine was collected in plastic tubes containing 200 μl acetic acid and stored at −70°C until analysis. Assays were performed within 6 months after collection; these analytes are stable under those storage conditions. Kågedal et al. (1992) have also shown that urinary concentrations of 5-*S*-CD and 6H5MI2C do not change in 2 months at −20°C. A total of 108 serum and urine samples were collected for this study, but one subject had an unusually high serum and urinary levels of 5-*S*-CD in March (serum level 13.0 nmol/l; urinary level 92.5 μmol/mol creatinine). The reason for these high values is not known. Another subject also had a level of serum 5-*S*-CD (14.3 nmol/l) exceeding the cut-off value of 10.0 nmol/l (Wakamatsu et al., 1991). The level may be due to a hiking 1 week earlier. Therefore, those serum and corresponding urine samples were excluded from evaluation. In Japan, March is the first month when UVB radiation increases considerably (33% increase from February in our case), and we occasionally observe a jump in serum 5-*S*-CD levels 1 week after outside activity.

Data for solar UVB radiation from sunlight were obtained from National Institute of Vegetable and Tea Science, Taketoyo, Aichi, located 30 km south of Toyoake, Aichi, where the nine subjects spent their daytime during weekdays.

Determination of levels of 5-*S*-CD and 6H5MI2C in the serum and urine

Determination of 5-*S*-CD in specimens was performed using HPLC with electrochemical detection, as previously reported (Wakamatsu

and Ito, 1994). Determination of 6H5MI2C in the serum and urine was performed using HPLC as previously reported (Wakamatsu et al., 1991) but using a fluorescence detector, JASCO FP-2020, instead of the originally described electrochemical detector. The excitation wavelength was 315 nm and the emission wavelength was 420 nm. We also used a filtration device (Alltech Associates, Inc., Deerfield, IL, USA). Levels of urinary analytes were calculated against creatinine, as described by Kärnell et al. (2000).

Statistical analysis

Statistical testing was carried out using JMP 5.0 for Macintosh (SAS Institute, Tokyo, Japan; http://www.jmp.com/japan/corp/index.shtml). Differences were analysed for statistical significance using the non-parametric Mann–Whitney *U*-test. P-values < 0.05 are considered to be significant.

Acknowledgements

This study was supported in part by a Grant-in-Aid for Scientific Research (no. 16591122) from the Ministry of Education, Culture, Sports and Technology of Japan, and for Cancer Research (15–10) from the Ministry of Health, Labour and Welfare.

References

Agrup, G., Hansson, C., Rorsman, C., Rosengren, A.-M., Rosengren, E., and Tegner, E. (1978). 5-*S*-cysteinyldopa excretion after treatment with 8-methoxypsoralen and UVA light. J. Invest. Dermatol. *70*, 25–26.

Agrup, G., Agrup, P., Andersson, T., Hafström, L., Hansson, C., Jacobsson, S., Jönsson, P.-E., Rorsman, H., Rosengren, A.-M., and Rosengren, E. (1979). 5 yr' experience of 5-S-cysteinyldopa in melanoma diagnosis. Acta Derm. Venerol. *59*, 381–388.

Ekelund, M.C., Carstam, R., Hannson, C., Rorsman, H., and Rosengren, E. (1985). Urinary excretion of 5-S-cysteinyldopa and 6-hydroxyindole-2-carboxylic acid: differences between pigmented and albino mice. Acta Derm. Venereol. *65*, 437–439.

Hansson, C. (1988). Some indolic compounds as markers of the melanocyte activity. Acta Derm. Venereol. Suppl. *138*, 1–60.

Hansson, C., Rorsman, H., Rosengren, E., and Tegner, T. (1981). 5-S-Cysteinyldopa and dopa in serum during treatment with 8-methoxypsoralen and UVA light. Acta Derm. Venereol. *61*, 251–255.

Hearing, V.J. (1998). The regulation of melanin production. In The Pigmentary System. Physiology and Pathophysiology, J.J. Nordlund, R.E. Boissy, V.J. Hearing, R.A. King, J.-P. Ortonne, ed. (New York: Oxford University Press), pp. 423–438.

Ito, S. (2003). A chemist's view of melanogenesis. Pigment Cell Res. *16*, 230–236.

Kågedal, B., Lenner, L., Årstrand, K., and Hansson, C. (1992). The stability of 5-*S*-cysteinyldopa and 6-hydroxy-5-methoxyindole-2-carboxylic acid in human urine. Pigment Cell Res. *5* (Suppl. 2), 304–307.

Kärnell, R., Kågedal, B., Lindholm, C., Nilsson, B., Årstrand, K., and Ringborg, U. (2000). The value of cysteinyldopa in the follow-up of disseminated malignant melanoma. Melanoma Res. *10*, 363–369.

Matsumura, Y., and Anathaswamy, H.N. (2004). Toxic effects of ultraviolet radiation on the skin. Toxicol. Appl. Pharmacol. *195*, 298–308.

Meyerhöffer, S., Lindberg, Z., Häger, A., Kågedal, B., and Rosdahl, I. (1998). Urinary excretion of 5-*S*-cysteinyldopa and 6-hydroxy-5-methoxyindole-2-carboxylic acid in children. Acta Derm. Venereol. *78*, 31–35.

Nimmo, J.E., Gawkrodger, D.J., O'Docherty, C.S.J., Going, S.M., Percy-Robb, I.W., and Hunter, J.A.A. (1988). Plasma 5-*S*-cysteinyldopa as an index of melanogenesis. Brit. J. Dermatol. *118*, 487–496.

Rodgers, K.J., and Dean, R.T. (2000). Metabolism of protein-bound DOPA in mammals. Int. J. Biochem. Cell Biol. *32*, 945–955.

Rorsman, H., Agrup, G., Falck, B., Rosengren, A.M., and Rosengren, E. (1976). Exposure to sunlight and urinary excretion of 5-*S*-cysteinyldopa. In Pigment Cell, Vol. 2, V. Riley, ed. (Basel: Karger), pp. 284–289.

Stierner, U. (1991). Melanocytes, moles and melanoma – a study on UV effects. Acta Derm Venereol. Suppl. *168*, 1–31.

Stierner, U., Rosdahl, I., Augustsson, A., and Kågedal, B. (1988). Urinary excretion of 5-*S*-cysteinyldopa in relation to skin type, UVB-induced erythema, and melanocyte proliferation in human skin. J. Invest. Dermatol. *91*, 506–510.

Tegner, E., Rorsman, H., and Rosengren, E. (1983). 5-*S*-Cysteinyldopa and pigment response to UVA light. Acta Derm. Venereol. *63*, 21–25.

Wakamatsu, K., and Ito, S. (1990). Identification of ester glucuronide and sulfate conjugates of 5-hydroxy-6-methoxyindole-2-carboxylic acid and 6-hydroxy-5-methoxyindole-2-carboxylic acid in melanoma urine. J. Dermatol. Sci. *1*, 253–260.

Wakamatsu, K., and Ito, S. (1994). Improved HPLC determination of 5-*S*-cysteinyldopa in serum. Clin. Chem. *40*, 495–496.

Wakamatsu, K., and Ito, S. (1995). Seasonal variation in serum concentration of 5-*S*-cysteinyldopa and 6-hydroxy-5-methoxyindole-2-carboxylic acid in healthy Japanese. Pigment Cell Res. *8*, 132–134.

Wakamatsu, K., Ito, S., and Fujita, K. (1990). Production, circulation, and excretion of melanin-related metabolites in B16 melanoma-bearing mice. Acta Derm. Venereol. *70*, 367–372.

Wakamatsu, K., Ito, S., and Horikoshi, T. (1991). Normal values of urinary excretion and serum concentration of 5-*S*-cysteinyldopa and 6-hydroxy-5-methoxyindole-2-carboxylic acid, biochemical markers of melanoma progression. Melanoma Res. *1*, 141–147.

Wakamatsu, K., Kageshita, T., Furue, M. et al. (2002). Evaluation of 5-S-cysteinyldopa as a marker of melanoma progression: 10 yr' experience. Melanoma Res. *12*, 245–253.

Westerhof, W., Pavel, S., Kammeyer, A., Beusenberg, F.D., and Cormane, R. (1987). Melanin-related metabolites as markers of the skin pigmentary system. J. Invest. Dermatol. *95*, 78–81.

Wirestrand, L.-E., Hansson, C., Rosengren, E., and Rorsman, H. (1985). Melanocyte metabolites in the urine of people of different skin colour. Acta Derm. Venereol. *65*, 345–348.

PNAS
Proceedings of the National Academy of Sciences of the United States of America www.pnas.org

Encapsulation of a reactive core in neuromelanin

Shosuke Ito

PNAS published online Sep 27, 2006;
doi:10.1073/pnas.0606879103

Encapsulation of a reactive core in neuromelanin

Shosuke Ito*

Department of Chemistry, Fujita Health University School of Health Sciences, Toyoake, Aichi 470-1192, Japan

Melanin pigments are found widely in animals and plants (1). Melanin's most conspicuous presence is on the surface of the body, where it serves to protect underlying tissues from harmful UV radiation and to camouflage the organism from enemies. Two chemically distinct types of melanin pigments are produced in the melanocytes of mammals and birds: the black-to-brown eumelanin and the yellow-to-reddish-brown pheomelanin. Biochemical pathways to these melanin pigments are now well clarified (1, 2). Both pigments are derived from a common precursor, dopaquinone (DQ), which is formed from the amino acid tyrosine upon oxidation with a specialized enzyme, tyrosinase. DQ is a highly reactive intermediate that, after cyclization, undergoes a complex series of redox reactions leading to the production of eumelanin, a highly heterogeneous polymer consisting of 5,6-dihydroxyindole and 5,6-dihydroxyindole-2-carboxylic acid. On the other hand, when cysteine intervenes in this pathway, it gives rise to cysteinyldopa isomers that, upon oxidation, lead to pheomelanin production via benzothiazine intermediates (see ref. 2 for the pathway of mixed melanogenesis). A brown, insoluble, melanin-like pigment also is found in the central nervous system of humans and primates (3). This pigment, termed neuromelanin (NM), is present in highest concentration in catecholaminergic neurons of the substantia nigra and locus ceruleus regions of the midbrain. In recent years, research on NM has attracted much attention because of its possible role in the pathogenesis of Parkinson's disease. In contrast to the cutaneous melanin, however, much less is known about the structure and function of NM because of difficulty with isolation and lack of adequate biosynthetic models (3). In this issue of PNAS, Bush *et al.* (4) have shown by employing sophisticated physical methods, in particular photoelectron emission microscopy (PEEM) coupled to a free-electron laser (FEL) (5), that NM is composed of granules with ≈30-nm diameters consisting of pheomelanin at the core and eumelanin at the surface.

Casing Model of Mixed Melanogenesis

In a previous work (6), the same group used the FEL–PEEM technique to establish that human eumelanosomes from black hair have a surface oxidation potential of −0.2 V vs. the normal hydrogen electrode. On the other hand, human melanosomes from red hair contain a mixture of eumelanin and pheomelanin, which is reflected by oxidation potentials of −0.2 and +0.5 V, respectively. Because FEL–PEEM is a surface technique, the results indicate that melanosomes from red hair have both types of melanin on or near their surface. Chemical degradation of NM shows that this pigment also is composed of both eumelanic and pheomelanic components in a ratio of 3–4 to 1 (7). But the application of FEL–PEEM to NM granules isolated from human brains (4) reveals a single oxidation potential (−0.1 V), indicating the presence of only eumelanin on the surface; no pheomelanic species are detected on or near the surface of the NM granules. Therefore, an explanation is needed for how the eumelanin surface is built up on the pheomelanin core.

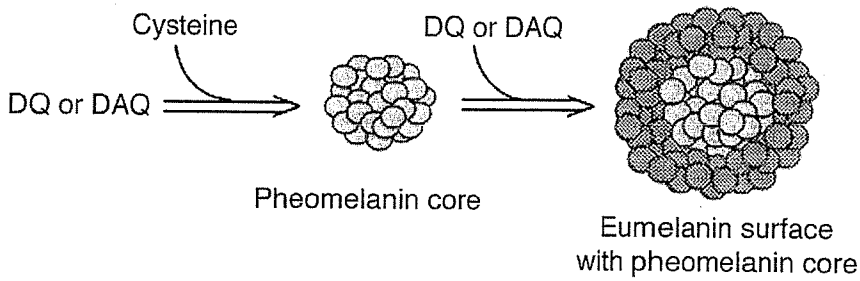

Fig. 1. Casing model of mixed melanogenesis. In the process of mixed melanogenesis, pheomelanic pigment is produced first, followed by deposit of eumelanic pigment. In the granule with the eumelanin surface, the side is intentionally cut away to reveal the inner pheomelanin core.

Kinetic studies on the fate of DQ in the presence or absence of cysteine have clearly indicated that pheomelanin production is favored over eumelanin production as long as cysteine concentration is >1 μM (2, 8). This favored production of pheomelanin suggests that, in the process of mixed melanogenesis, pheomelanin is always formed first, and then eumelanin is deposited on the preformed pheomelanin (Fig. 1). This casing model was originally suggested by Agrup *et al.* (9), based on biochemical findings. Now, the work by Bush *et al.* (4) provides biophysical evidence supporting this model. In NM production, this casing process is further favored by the fact that dopaminequinone (DAQ) cyclizes ≈100-fold more slowly than DQ (2), leading to a preferential production of cysteinyldopamine followed by oxidation to pheomelanic pigment.

Implications of Architecture of NM

The physiological and pathological roles of NM in the dopaminergic neurons are not well understood (3). Nevertheless, the present study by Bush *et al.* (4) makes several intriguing interpretations possible for the roles of NM. First, the neurotoxicity of dopamine may be explained by the casing model (Fig. 1). Dopamine is known to be highly cytotoxic to neuronal cells, where it is oxidized under oxidative stress to DAQ, the ultimate toxic intermediate (10). As the kinetic data (2, 8) indicate, in neurons, DAQ rapidly conjugates with cysteine to form cysteinyldopamine isomers. In fact, the highest levels of 5-*S*-cysteinyldopamine among various brain tissues, although in trace concentrations (<100 nM), were detected in the substantia nigra (11). This mechanism could serve to detoxify the harmful DAQ intermediate. If DAQ is not scavenged by reaction with cysteine, then it may bind to neuroprotective proteins, such as parkin, through the cysteine residues to form cysteinyldopamine–protein adducts, thereby exerting neurotoxicity (10).

The casing model (Fig. 1) of NM architecture indicates that, in dopaminergic neurons of the substantia nigra, NM synthesis is kinetically regulated in such a manner that DAQ is conjugated first with cysteine to form cysteinyldopamine

Author contributions: S.I. wrote the paper.

The author declares no conflict of interest.

See companion article on page 14785.

*E-mail: sito@fujita-hu.ac.jp.

isomers, which are oxidized by DAQ through a redox reaction to form a pheomelanic core. This reaction is followed by the production of a eumelanic surface by a series of spontaneous reactions of DAQ, leading to the detoxification of DAQ. The extremely low content of cysteine in substantia nigra neurons is consistent with this view (12).

Second, the casing model may be relevant to protection against the development of Parkinson's disease, a common neurodegenerative disorder with clinical features that include tremor, slowness of movement, and stiffness. In Parkinson's disease, a selective loss of highly pigmented dopaminergic neurons in the substantia nigra occurs, whereas less-pigmented neurons are spared (13). Although exact mechanisms underlying this phenomenon are still under extensive investigation, NM is believed to play a neuroprotective role by binding toxic organic molecules and redox-active metal ions, especially iron (3). The interaction between iron and NM has been a focus of intensive research (14), because a marked accumulation of iron in parallel with disease severity is reported in the parkinsonian substantia nigra. NM is only partially saturated with iron in a healthy brain, thus playing a physiological role in intraneuronal iron homeostasis. The casing model (Fig. 1) is relevant in this respect in that pheomelanin is less efficient than eumelanin in binding drugs and metal ions (15). If pheomelanin were at the surface, the neuroprotective role of NM would not be expected.

Another possible implication of the casing model (Fig. 1) is related to the prooxidant property of pheomelanin. Ye *et al.* (16) have shown that, even in the absence of light, pheomelanin is able to reduce molecular oxygen at an appreciable rate, which is a property not observed with eumelanin. As one possible mechanism for the selective loss of dopaminergic neurons in Parkinson's disease, it has been proposed that the saturation of iron-binding sites caused by high iron levels leads to an increase in cytosolic, redox-active iron and subsequent cellular damage (17). Increased oxidative stress under such conditions could result in degradation of the eumelanic surface of NM by reactive oxygen species, thus exposing the pheomelanic core that is not only ineffective in iron binding but also behaves as a prooxidant itself. This exposure of pheomelanic core would lead to a vicious circle of neurodegenerative events in the parkinsonian substantia nigra. In fact, the iron-binding ability of NM in the parkinsonian brain is reduced compared with that in the healthy brain (17).

The casing model (Fig. 1) has not attracted much attention among pigment cell researchers. The past two decades have witnessed great progress in melanin research, especially regarding the biosynthesis and functions of eumelanin and pheomelanin (1, 2). The work by Bush *et al.* (4) now points out the significance of looking at the surface properties of melanosomes, i.e., whether they are eumelanic, pheomelanic, or both. Interest in NM has been increasing steadily over the years but has been hampered by the difficulty with isolation of NM and the scanty information on its structure. The architecture of NM granules proposed by Bush *et al.* (4) not only would make interpretation of the existing vast amounts of information on NM possible but also should stimulate renewed interest in the roles of NM in the pathogenesis of Parkinson's disease, the second-most-prevalent neurodegenerative disorder.

1. Nordlund JJ, Boissy RE, Hearing VJ, King RA, Oetting WS, Ortonne JP, eds (2006) *The Pigmentary System: Physiology and Pathophysiology* (Blackwell, Oxford), 2nd Ed.
2. Ito S (2003) *Pigment Cell Res* 16:230–236.
3. Fedorow H, Tribl F, Halliday G, Gerlach M, Riederer P, Double KL (2005) *Prog Neurobiol* 75:109–124.
4. Bush WD, Garguilo J, Zucca FA, Albertini A, Zecca L, Edwards GS, Nemanich RJ, Simon JD (2006) *Proc Natl Acad Sci USA* 103:14785–14789.
5. Samokhvalov A, Garguilo J, Yang WC, Edwards GS, Nemanich RJ, Simon JD (2004) *J Phys Chem B* 108:16334–16338.
6. Samokhvalov A, Hong L, Liu Y, Garguilo J, Nemanich RJ, Edwards GS, Simon JD (2005) *Photochem Photobiol* 81:145–148.
7. Wakamatsu K, Fujikawa K, Zucca FA, Zecca L, Ito S (2003) *J Neurochem* 86:1015–1023.
8. Land EJ, Ito S, Wakamatsu K, Riley PA (2003) *Pigment Cell Res* 16:487–493.
9. Agrup G, Hansson C, Rorsman H, Rosengren E (1982) *Arch Dermatol Res* 272:103–115.
10. LaVoie MJ, Ostaszewski BL, Weihofen A, Schlossmacher MG, Selkoe DJ (2005) *Nat Med* 11:1214–1221.
11. Spencer JPE, Jenner P, Daniel SE, Lees AJ, Marsden DC, Halliwell B (1998) *J Neurochem* 71:2112–2122.
12. Aoyama K, Suh SW, Hamby AM, Liu J, Chan WY, Chen Y, Swanson RA (2006) *Nat Neurosci* 9: 119–126.
13. Kastner A, Hirsch EC, Lejeune F, Javoy-Agid F, Rascol O, Agid Y (1992) *J Neurochem* 59:1080–1089.
14. Zecca L, Youdim MBH, Riederer P, Connor JR, Crichton RR (2004) *Nat Rev Neurosci* 5:863–873.
15. Mårs U, Larsson BS (1999) *Pigment Cell Res* 12:266–272.
16. Ye T, Hong L, Garguilo J, Pawlak A, Edwards GS, Nemanich RJ, Sarna T, Simon JD (2006) *Photochem Photobiol* 82:733–737.
17. Fasano M, Bergamasco B, Lopiano L (2006) *J Neurochem* 96:909–916.

Traffic 2006; 7: 1–14
Blackwell Munksgaard

doi: 10.1111/j.1600-0854.2006.00431.x

Interaction of Hermansky-Pudlak Syndrome Genes in the Regulation of Lysosome-Related Organelles

Rashi Gautam[1], Edward K. Novak[1], Jian Tan[1], Kazumasa Wakamatsu[2], Shosuke Ito[2] and Richard T. Swank[1,*]

[1]*Department of Molecular and Cellular Biology, Roswell Park Cancer Institute, Elm & Carlton Sts., Buffalo, NY 14263, USA*
[2]*Department of Chemistry, Fujita Health University School of Health Sciences, Toyoake, Aichi 470-1192, Japan*
** Corresponding author: Richard T. Swank, richard.swank@roswellpark.org*

Hermansky-Pudlak Syndrome (HPS) is a genetically heterogeneous disease caused by abnormalities in the synthesis and/or trafficking of lysosome-related organelles (LROs) including melanosomes, lamellar bodies of lung type II cells and platelet dense granules. At least 15 genes cause HPS in mice, with a significant number specifying novel subunits of protein complexes termed BLOCs (*B*iogenesis of *L*ysosome-related *O*rganelles Complexes). To ascertain whether BLOC complexes functionally interact *in vivo*, mutant mice doubly or triply deficient in protein subunits of the various BLOC complexes and/or the AP-3 adaptor complex were constructed and tested for viability and for abnormalities of melanosomes, lung lamellar bodies and lysosomes. All mutants, including those deficient in all three BLOC complexes, were viable though the breeding efficiencies of multiple mutants involving AP-3 were severely compromised. Interactions of BLOC protein complexes with each other and with AP-3 to affect most LROs were apparent. However, these interactions were tissue and organelle dependent. These studies document novel biological interactions of BLOC and AP-3 complexes in the biosynthesis of LROs and assess the role(s) of HPS protein complexes in general health and physiology in mammals. Double and triple mutant HPS mice provide unique and practical experimental advantages in the study of LROs.

Key words: dense granule, gene, lamellar body, lysosome, melanosome, mutant, vesicle

Received 8 February 2006, revised and accepted for publication 22 March 2006

Lysosome-related organelles (LROs) traffic through the endocytic pathway, share a subset of membrane proteins, are acidic and are relatively high in calcium (1–3). Numerous intracellular granules belong to this class though the most commonly studied LROs are melanosomes, platelet dense granules, cytotoxic T lymphocyte (CTL), granules and lamellar bodies of lung type II cells.

The molecular identifications of mutations causative for inherited diseases such as Hermansky-Pudlak Syndrome (HPS) (4–6), Chediak–Higashi Syndrome (7,8) and Griscelli Syndrome (9) have revealed genes and proteins important for the regulation of the synthesis of LROs. Hermansky-Pudlak Syndrome is a genetically heterogeneous disease with 8 causative genes identified thus far in humans (5,10) and at least 15 in mouse models (3). Mutations in these genes cause hypopigmentation, prolonged bleeding times and lung disease due to abnormal synthesis and/or vesicular trafficking of melanosomes, platelet dense granules and lamellar bodies, respectively. Associated clinical issues may include visual deficiencies and hypopigmentation, hemorrhaging requiring repeated platelet transfusions, fatal fibrotic lung disease and, in selected cases, increased susceptibility to infections and granulomatous colitis.

The majority (10) of the 15 murine HPS proteins exist together with other HPS proteins in three protein complexes termed Biogenesis of Lysosome-related Organelles Complexes (BLOCs) (3,11). A fascinating aspect of these 10 proteins is that all are novel and are found only in higher vertebrates. Their sequences offer few clues to their functions or to the mechanisms by which the BLOCs orchestrate the biogenesis and trafficking of LROs. Proteins encoded by the *pallid, muted, sandy* (*HPS7*), *cappuccino* and *reduced pigmentation* (*HPS8*) HPS genes together with three additional novel subunits are part of BLOC-1. BLOC-2 is composed of proteins encoded by the *cocoa* (*HPS3*), *ruby-eye 2* (*HPS5*) and *ruby-eye* (*HPS6*) genes. BLOC-3 contains proteins encoded by the *pale ear* (*HPS1*) and *light ear* (*HPS4*) genes. Four other HPS proteins are well known to mediate vesicle trafficking to and among LROs. Two, altered in the pearl and mocha HPS mouse mutants, respectively, are the β_3A (*HPS2*) and δ subunits of the AP-3 adaptor complex (12), which mediate the sorting of membrane proteins to LROs. The alpha subunit of the rab geranylgeranyl transferase complex and the VPS33a protein are altered in the gunmetal and buff mutants, respectively. Finally, the xCT cystine/glutamate transporter is not expressed in the subtle gray mutant (13).

It is well known that the 10 novel HPS proteins within each BLOC complex interact directly with other members of that complex. In contrast, there are no indications from classical approaches, such as yeast two-hybrid or co-immunoprecipitation, that proteins of different BLOC complexes or the AP-3 complex directly interact. Nevertheless,

it is possible that these complexes do interact indirectly to orchestrate the synthesis and trafficking of LROs. One method to detect such indirect interactions is the genetic or epistasis approach (14,15), by examining the phenotypes of mutants that contain mutations in multiple mutant genes. An added value of multiple mutants is that they may present with more severe phenotypes than single mutants (16,17). These more severe 'clinical' phenotypes may reveal novel physiological functions of these genes and may be advantageous for the design and testing of new therapies (17). The more severe phenotypes of the multiple mutants may be the more appropriate models for severe forms of the human disease, than single mutants (17,18). A more fundamental question is whether multiple HPS mutations are viable. The present epistasis studies were designed to comprehensively assess the viability of multiple HPS mutants and the extent of indirect interaction *in vivo* between the various HPS BLOCs and the AP-3 complex in the synthesis and/or function of LROs.

Results

General health and breeding issues

In total, 11 multiple mutants involving all possible combinations of BLOC and AP-3 complexes (Table 1) were produced by appropriate matings of single mutants. Double mutants deficient in all possible combinations of the three BLOC complexes (Figure 1), produced at efficiencies expected for Mendelian genes, were viable and in fact appeared healthy. Notably, triple mutants, deficient in all three BLOC complexes, were viable and healthy for at least nine months of age. Body weights of multiple mutants involving all BLOC complexes were not significantly different from those of control C57BL/6J mice between the ages of 3 and 12 weeks (Figure 2). Similarly, double and triple mutants involving all combinations of AP-3 together with the BLOC complexes were viable (Figure 1). However, the ability to produce multiple mutants deficient in AP-3 together with any of the various BLOCs was considerably reduced compared to mutants deficient in multiple BLOC complexes. For example, at the last stage of the process of producing the quadruple mutant BLOC-1^{-}, 2^{-}, 3^{-}, AP-3^{-}, we observed just 2 quadruple mutant offspring among 85 total offspring despite the prediction of 21 quadruple mutants by the laws of Mendelian genetics. Similarly, low production of other multiple mutants deficient in AP-3 and various BLOCs mutants were observed. A practical result of this difficulty in obtaining multiple mutants involving AP-3 was a significant limitation of analyses of LRO abnormalities in these mutants (see below).

Similarly, there was a major difference (Table 2) in breeding efficiencies of homozygous multiple mutants involving the BLOC complexes as compared to those involving AP-3 together with the various BLOCs. The breeding ability of mutants deficient in multiple BLOC complexes was uncompromised as compared with that of C57BL/6J. In fact homozygous BLOC-1^{-}, 2^{-}, 3^{-} mutants, deficient in all three BLOC complexes interbred normally. In contrast, a large drop (40–60%) in breeding efficiency was apparent in all multiple mutants deficient in the AP-3 complex and any one of the BLOC complexes (though the breeding efficiency of homozygous AP-3 single mutants was uncompromised). Normal litter sizes were obtained when either male or female BLOC-3^{-}, AP-3^{-} homozygotes were bred to C57BL/6J (not shown). This indicates the AP-3 mediated loss in breeding efficiency is unlikely to be caused by specific abnormalities in either sperm or egg production, but rather is due to a general inefficiency in zygote production and/or development.

Pigmentation and melanosomes

Perhaps the most sensitive, certainly the most visually apparent, effects of the HPS genes are on pigmentation of the coat and eyes.

Coat color

Double mutants involving BLOC-1 together with either BLOC-2 or BLOC-3 have coat colors indistinguishable from that of the single BLOC-1 mutant (Figure 1). Likewise, the coat color of the BLOC-1^{-}, 2^{-}, 3^{-} triple mutant is indistinguishable from BLOC-1^{-} (Figure 1). This

Table 1: Affected protein complexes and genotypes of multiple mutant mice deficient in BLOCs and AP-3

Mutants	Affected vesicle protein complex	Genotype
BLOCs	BLOC-1^{-}, 2^{-}	$Pldn^{pa}/Pldn^{pa}$, $Hps6^{ru}/Hps6^{ru}$
	BLOC-1^{-}, 3^{-}	$Pldn^{pa}/Pldn^{pa}$, $Hps1^{ep}/Hps1^{ep}$
	BLOC-2^{-}, 3^{-}	$Hps3^{coa}/Hp^{coa}$, $Hps4^{le}/Hps4^{le}$
	BLOC-1^{-}, 2^{-}, 3^{-}	$Pldn^{pa}/Pldn^{pa}$, $Hps5^{ru2-J}/Hps5^{ru2-J}$, $Hps1^{ep}/Hps1^{ep}$
BLOCs & AP-3	BLOC-1^{-}, AP-3^{-}	$Pldn^{pa}/Pldn^{pa}$, $Ap3b1^{pe}/Ap3b1^{pe}$
	BLOC-2^{-}, AP-3^{-}	$Hps5^{ru2-J}/Hps5^{ru2-J}$, $Ap3b1^{pe}/Ap3b1^{pe}$
	BLOC-3^{-}, AP-3^{-}	$Hps1^{ep}/Hps1^{ep}$, $Ap3b1^{pe}/Ap3b1^{pe}$
	BLOC-1^{-}, 2^{-}, AP-3^{-}	$Pldn^{pa}/Pldn^{pa}$, $Hps6^{ru}/Hps6^{ru}$, $Ap3b1^{pe}/Ap3b1^{pe}$
	BLOC-1^{-}, 3^{-}, AP-3^{-}	$Pldn^{pa}/Pldn^{pa}$, $Hps1^{ep}/Hps1^{ep}$, $Ap3b1^{pe}/Ap3b1^{pe}$
	BLOC-2^{-}, 3^{-}, AP-3^{-}	$Hps5^{ru2-J}/Hps5^{ru2-J}$, $Hps1^{ep}/Hps1^{ep}$, $Ap3b1^{pe}/Ap3b1^{pe}$
	BLOC-1^{-}, 2^{-}, 3^{-}, AP-3^{-}	$Pldn^{pa}/Pldn^{pa}$, $Hps5^{ru2-J}/Hps5^{ru2-J}$, $Hps1^{ep}/Hps1^{ep}$, $Ap3b1^{pe}/Ap3b1^{pe}$

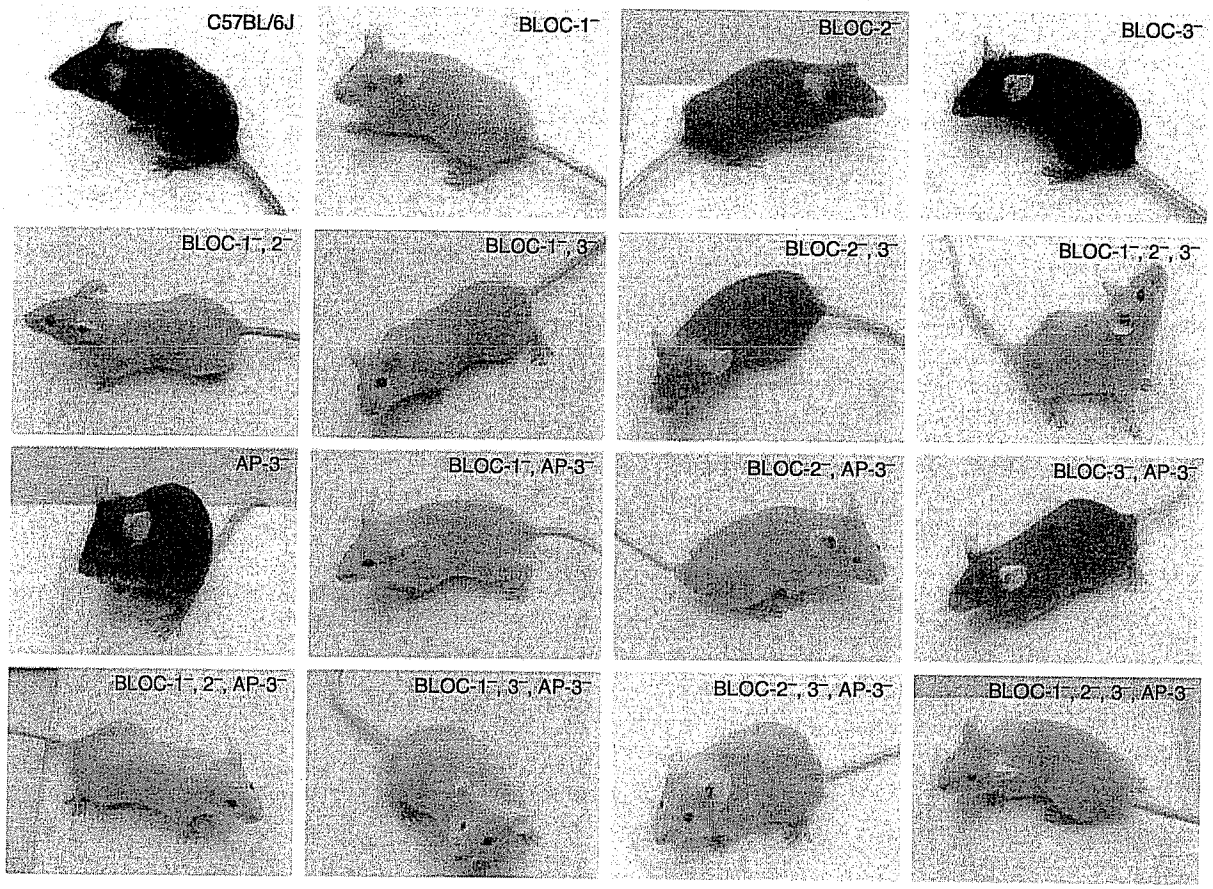

Figure 1: Single, double, triple and quadruple mutant HPS mice. Mutant mice together with strain-of-origin C57BL/6J are illustrated. All are 6–10 weeks of age.

suggests that these genes act on the same pathway, and that the BLOC-1 complex functions at an early stage of that pathway. The double mutant deficient in BLOC-2 and BLOC-3, however, is noticeably lighter than either single mutant in both coat and eye color, suggesting that these genes must also interact on an additional pathway. All double and triple mutants deficient in AP-3 and any other combinations of the three BLOCs are lighter in pigmentation than any single mutant. This diminution in pigmentation in the cases of all multiple mutants involving AP-3 and BLOC-1 is very subtle, requiring very close side-by side comparison of single and multiple mutants.

Eye color

Among the single BLOC mutants, the eye color of the BLOC-1$^-$ mutant is red, BLOC-2$^-$ eyes are dark red (ruby) and BLOC-3$^-$ eyes are black (Figure 1). All double and triple mutants involving BLOC-1 retain the red eye color of the BLOC-1$^-$ single mutant. The eye color of the double mutant BLOC-2$^-$, 3$^-$ is also red, that is, lighter than both single mutants. Thus similarly to coat color, eye color shows that BLOC-2 and BLOC-3 genes interact in an additional pathway.

The eye color of the single mutant AP-3$^-$ is black while the eyes of all double, triple and quadruple mutants involving BLOCs and AP-3 are the same red hue observed in the BLOC-1$^-$ single mutant (Figure 1). This result indicates that the AP-3 and BLOC-2 and BLOC-3 gene products interact and likely function in separate pathways in regulating eye pigmentation.

Chemical analyses of melanin

To place these visual observations on a more quantitative basis, melanin levels in hair were chemically determined (19,20) (Table 3). The degree of loss of total melanin confirmed visual conclusions. As expected, total melanin levels were significantly lower in hair of all mutants (except BLOC-3$^-$) than in control C57BL/6J. Total melanin levels, as expected, are very low in BLOC-1$^-$ and remain very low in all multiple mutants involving BLOC-1. Melanin levels of the BLOC-2$^-$, 3$^-$ double mutant are similar to that of the BLOC-2$^-$ mutant (though by visual examination the former is slightly more hypopigmented than the latter). As indicated above, loss of AP-3 accentuates the loss of melanin in all BLOC mutants by visual observation. However, the subtle effects of the AP-3 mutation on

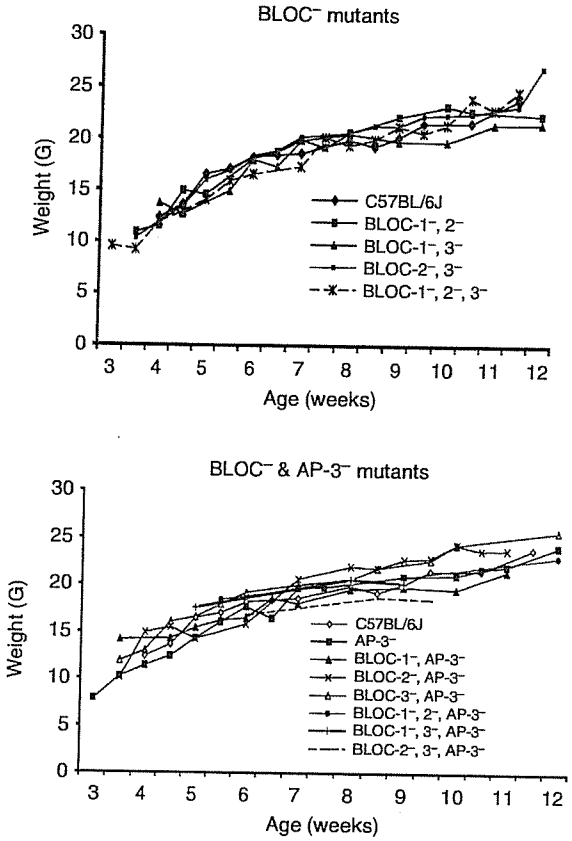

Figure 2: Body weights of multiple mutants. Three to six mice were analyzed per time point.

melanin levels of BLOC-1⁻ mutants are difficult to evaluate by chemical analysis since melanin levels are already extremely low in mutants deficient in BLOC-1. Nevertheless, a deficiency of AP-3 clearly causes a major loss of melanin of BLOC-2⁻ mutants and significantly, though less drastically, reduces melanin levels of BLOC-3⁻ mutants.

Table 2: Breeding efficiencies of multiple mutants

Genotype	Mean litter size	*n*	p value (vs. C57BL/6J)
C57BL/6J	6.4 ± 0.5	57	
BLOC-1⁻, 2⁻	5.5 ± 0.4	71	0.157
BLOC-1⁻, 3⁻	5.3 ± 0.3	66	0.054
BLOC-2⁻, 3⁻	6.3 ± 0.4	68	0.875
BLOC-1⁻, 2–3⁻	6.1 ± 0.6	13	0.784
AP-3⁻	5.4 ± 0.5	12	0.375
BLOC-1⁻, AP-3⁻	2.6 ± 0.3	16	0.0002[a]
BLOC-2⁻, AP-3⁻	3.8 ± 0.5	12	0.023[a]
BLOC-3⁻, AP-3⁻	3.3 ± 0.2	69	0.001[a]

Mean litter sizes were calculated from matings of homozygous × homozygous single or multiple mutants and compared with similar measurements on C57BL/6J. Matings of other homozygous × homozygous triple and quadruple matings involving AP-3 are not presented since so few of these homozygotes were available for breeding. *n* = number of litters analyzed.
[a]significant difference.

The great majority of mutant alterations in melanin occurs through loss of eumelanin (brown/black) pigment, the principal pigment of the non-agouti C57BL/6J strain, which is the background strain of the multiple mutants. However, it is intriguing that concentrations of hair pheomelanin (red/yellow) pigment moved in a direction opposite to that of eumelanin in many of the single and multiple mutants with the lowest total melanin levels (Table 3). In fact, most of these 'low melanin' mutants exhibited pheomelanin concentrations significantly higher than those of C57BL/6J.

Ultrastructure of eye melanosomes

Pigmentation is critically dependent upon the number and morphology of melanosomes. Ultrastructural examination of eye tissues is a sensitive method for detection of abnormalities of melanosomes. Quantitative and qualitative effects on melanosomes of the retinal pigment epithelium (RPE) and choroid occur in single BLOC mutants (3). Choroidal and RPE melanosomes are greatly reduced in quantity and are misshapen in the BLOC-1⁻ mutant pallid compared to those of C57BL/6J (Figure 3). The RPE melanosomes are fewer and misshapen while choroidal melanosomes are fewer, misshapen and characteristically clumped within multimelanosomal vesicles in the BLOC-2⁻ mutant ruby eye-2 (Figure 3). In the BLOC-3⁻ mutant pale ear, RPE melanosomes are fewer and misshapen and choroidal melanosomes are fewer and characteristically giant (Figure 3).

Significantly more drastic effects on eye melanosomes are apparent in all double and triple BLOC mutants, especially in the choroid (Figure 3). Melanosomes are reduced to very small numbers in both eye tissues in all multiple BLOC mutants involving BLOC-1, and those few remaining are misshapen. A clear qualitative interaction of the BLOC-2 and BLOC-3 genes to produce new types of melanosomes in the BLOC-2⁻, 3⁻ double mutant is apparent. Melanosomes of the RPE are partially melanized being overall much less dense than those of either single mutant. Also, these melanosomes have unusual small dense inclusions. Melanosomes of the choroid resemble those of the BLOC-2⁻ single mutant in size (giant melanosomes of the BLOC-3⁻ mutant are absent) and in a tendency for clumping or multimelanosomal body formation. However, they are less dense than those of either single mutant. The BLOC-1⁻, 2⁻, 3⁻ triple mutant has reduced melanosomes in both RPE and choroid compared to the double mutants.

The effects of mutation of the AP-3 complex on eye melanosomes are illustrated in Figure 4. Melanosomes of both RPE and choroid of AP-3⁻ single mutants (Figure 4) are significantly reduced in number, compared

Table 3: Melanin analyses (±SEM) of hair of double and triple HPS mutants

Samples	Eumelanin[a] (μg/mg)	Pheomelanin[b] (μg/mg)	Total melanin (μg/mg)
C57BL/6J	85.5 ± 5.26	0.305 ± 0.02	85.7 ± 5.28
BLOC-1$^-$	1.39 ± 0.23****	0.899 ± 0.27	2.28 ± 0.50****
BLOC-2$^-$	24.0 ± 0.45****	0.763 ± 0.10**	24.7 ± 0.55****
BLOC-3$^-$	76.7 ± 2.28	0.470 ± 0.21	77.1 ± 2.49
BLOC-1$^-$, 2$^-$	1.25 ± 0.21****	0.617 ± 0.25	1.86 ± 0.46****
BLOC-1$^-$, 3$^-$	1.21 ± 0.39****	0.990 ± 0.35	2.20 ± 0.74****
BLOC-2$^-$, 3$^-$	20.9 ± 2.76****	0.715 ± 0.14*	21.5 ± 2.90***
BLOC-1$^-$, 2$^-$, 3$^-$	1.51 ± 0.34****	1.28 ± 0.33*	2.78 ± 0.37****
AP-3$^-$	11.4 ± 1.20****	0.494 ± 0.13	11.8 ± 1.33****
BLOC-1$^-$, AP-3$^-$	0.87 ± 0.08****	0.772 ± 0.05***	1.64 ± 0.13****
BLOC-2$^-$, AP-3$^-$	1.90 ± 0.16****	0.657 ± 0.04***	2.55 ± 0.20****
BLOC-3$^-$, AP-3$^-$	12.0 ± 0.84****	0.860 ± 0.12**	12.8 ± 0.96****
BLOC-1$^-$, 3$^-$, AP-3$^-$	1.23 ± 0.56****	1.46 ± 0.26**	2.61 ± 0.82****
BLOC-2$^-$, 3$^-$, AP-3$^-$	1.39 ± 0.15****	1.46 ± 0.47*	2.84 ± 0.62****

[a]Eumelanin was obtained by multiplying the amount of PTCA by a conversion factor of 50 (19,20).
[b]Pheomelanin was obtained by multiplying the amount of 4-AHP by a conversion factor of 9 (19,20). Significance (P) values of data in columns 2–4 are derived by comparison to the C57BL/6J values. $n = 3$, *p = 0.05, **p = 0.02, ***p = 0.01, ****p = 0.001.

to C57BL6J (Figure 3). Interaction of AP-3 with all BLOC genes is apparent in the substantial reduction in the number of melanosomes of both eye tissues in all double mutants involving AP-3 and any of the BLOC components (Figure 4). Further, the number of multimelanosomal bodies in the choroid are increased in the BLOC-1$^-$, AP-3$^-$ and BLOC-3$^-$, AP-3$^-$ double mutants compared to each respective single mutant (Figure 4). Finally, the further loss of BLOC-3 in the BLOC-1$^-$, 3$^-$, AP-3$^-$ triple mutant (Figure 4) significantly reduces the number of RPE and choroidal melanosomes beyond those of any of the three single parental mutants.

Lung lamellar bodies

An LRO, the lamellar body of lung type II cells, is the principal reservoir of newly synthesized and circulating surfactant. We have analyzed lung phospholipids as a measure of lamellar body abnormalities in multiple mutants, as previous studies (17) demonstrated that an unusual accumulation of phospholipid accurately reflects surfactant accumulation in abnormal giant lamellar bodies of the double mutant, ep/pe (BLOC-3$^-$, AP-3$^-$).

As reported (17), there are little or no accumulations of p-lipids in lungs of any of the single HPS mutants (Figure 5). Also, we found no increases in certain double mutants (BLOC-1$^-$, 2$^-$ and BLOC- 2$^-$, 3$^-$). However, significant elevations of p-lipids were apparent in the BLOC-1$^-$, 3$^-$ double mutant and in the BLOC-1$^-$, 2$^-$, 3$^-$ triple mutant. It is striking that elevations of lung p-lipids occurred in all double mutants involving both AP-3 and BLOC complexes. A likely explanation for the increased p-lipid levels in these mutants is accumulation of surfactant in abnormal lamellar bodies, the LRO specific to lung type II cells (17). Indeed, specific identification of these LROs by surfactant protein B immunostaining (Figure 6) revealed greatly enlarged lamellar bodies with increased quantities of surfactant B in four multiple mutants with abnormal accumulation of lung p-lipids.

Because lung disease is the most critical clinical problem in HPS (17), additional studies were performed to determine the consequences of abnormal lamellar bodies in multiple HPS mutants. Studies with the BLOC-3$^-$, AP-3$^-$ double mutant (17,21) have led to the hypothesis that abnormalities in a critical LRO, the type II cell lamellar body, lead to infiltration of macrophages followed by overt lung disease (17,21). The accumulating macrophages secrete a battery of lytic enzymes and inflammatory cytokines, which in turn wound the lung parenchyma (22). To obtain an accurate quantitation of the accumulation of macrophages, levels of N-acetyl glucosaminidase, which is accepted as a surrogate marker for lung macrophage accumulation (23), were determined (Figure 7). Among multiple mutants restricted to deficiencies in BLOC components, macrophages did not accumulate [despite the elevated p-lipids (Figure 5) and enlarged lamellar bodies (Figure 6)] in BLOC-1$^-$, 3$^-$ and BLOC-1$^-$, 2$^-$, 3$^-$ mutants. In contrast, macrophages did accumulate in all multiple mutants involving AP-3 (except BLOC-2$^-$, AP-3$^-$).

Secretion of lysosomal enzymes

In humans with HPS, defects in the lysosomal organelle are manifest by an abnormal accumulation of ceroid pigment. In mouse HPS models, deficiency of trafficking of the lysosome have been noted in several lysosomal systems, including lowered secretion of lysosomal enzymes from kidney proximal tubule cells of the testosterone-treated mouse (24) and from peritoneal macrophages treated with amines (25). Macrophages respond to incubation with amines such as chloroquine, methylamine and ammonia by alkalinization of the interior of lysosomes, fusion of the lysosome with the plasma membrane and

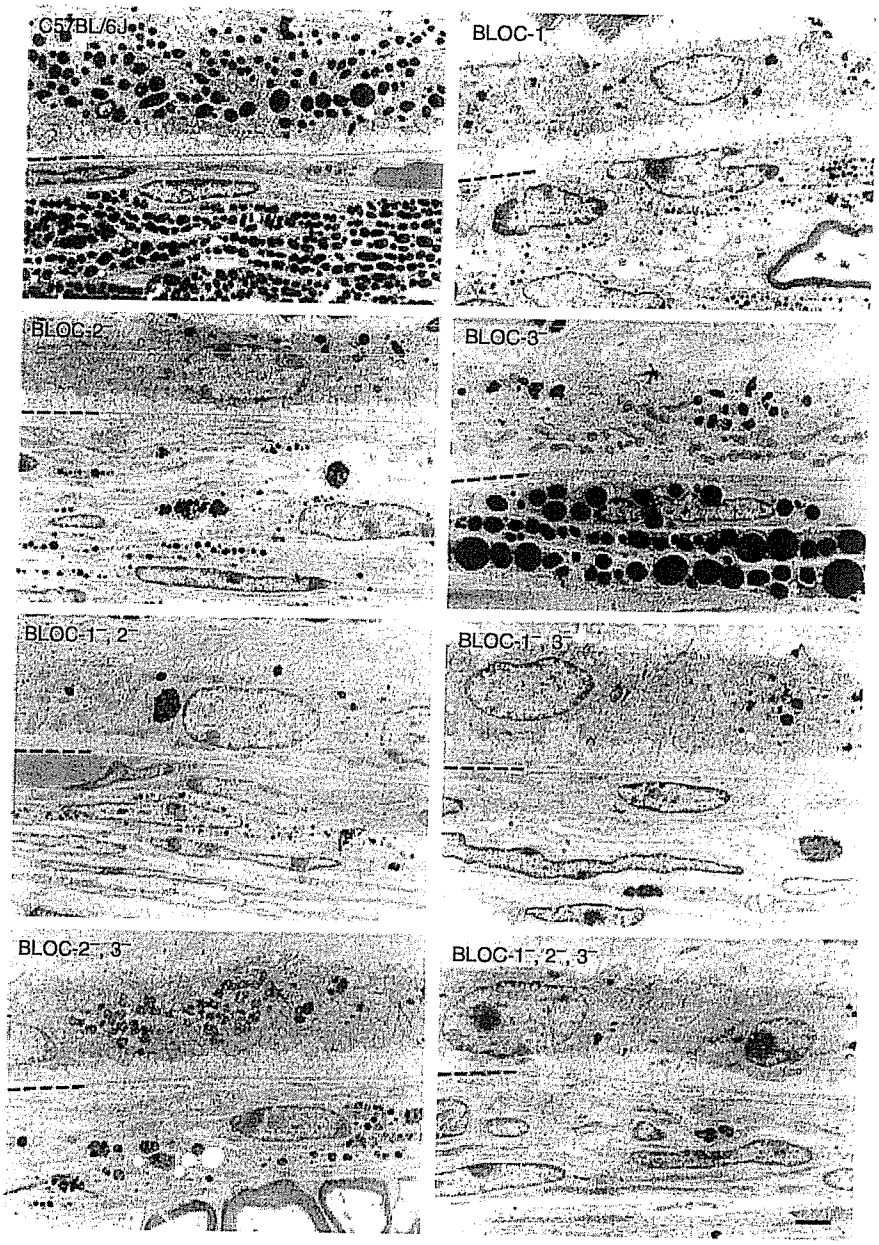

Figure 3: Ultrastructural analyses of melanosomes of the retinal pigment epithelium (RPE) and choroid in single and multiple HPS BLOC mutants. The interface between the RPE (above) and the choroid (below) is indicated in each case by a hyphenated partial line at left. Scale bar = 2 μm.

discharging massive quantities of mature lysosomal enzymes (25,26).

We had previously (25) documented that the pale ear (BLOC-3⁻) mutation caused significant reduction of secretion of lysosomal enzymes from ammonia-treated macrophages. This effect was specifically on mature (vesicular) rather than precursor lysosomal enzymes. Thus this system allows a comparison of the effects of multiple deficiencies of the various BLOC complexes on trafficking of the lysosomal organelle. It is striking that effects of deficiencies of the various single BLOCs on lysosomal enzyme secretion (Figure 8) differ from their effects on biogenesis of melanosomes (Figure 1). While deficiency of BLOC-1 causes by far the most severe effect on coat color and melanosome biogenesis, it has a minimal effect on lysosomal enzyme secretion (Figure 8). On the other hand, deficiency of BLOC-3 has minor effects on coat color (Figure 1) but causes a >50% loss in ability to secrete lysosomal enzymes (Figure 8). Deficiency of BLOC-2 has little or no effect on either LRO. Interactive effects are apparent in the minimal secretion observed in macrophages of the BLOC-2⁻, 3⁻ double mutant.

There was no effect of deficiency of AP-3 on lysosomal enzyme secretion. However, epistatic interaction was

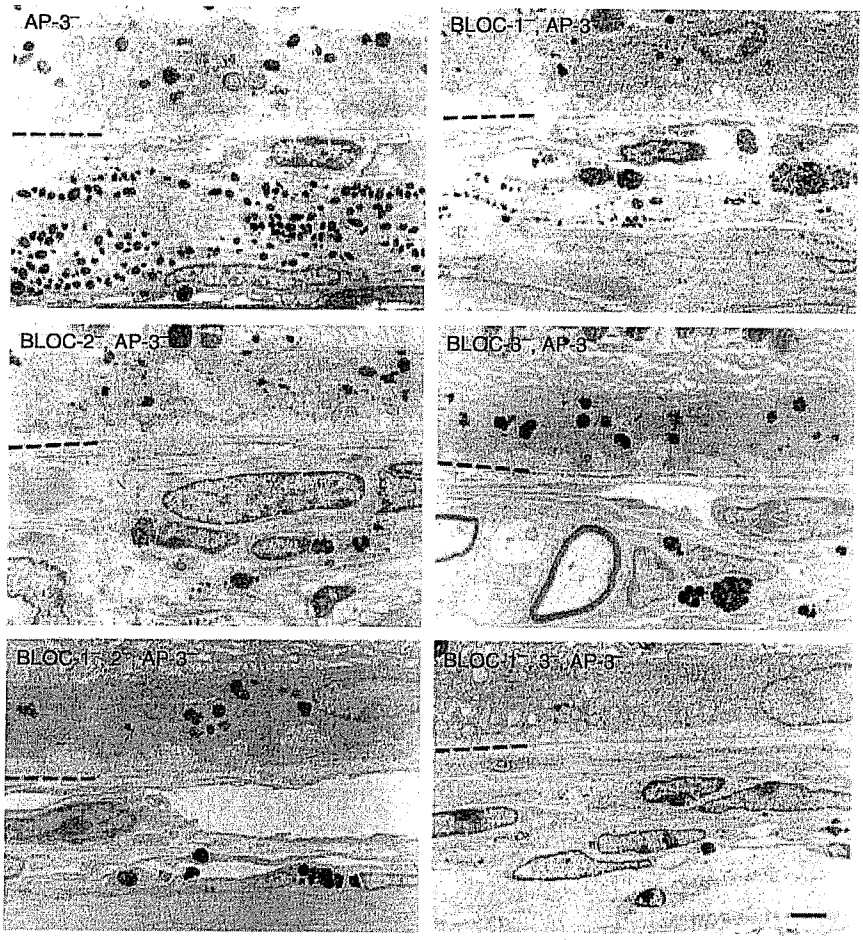

Figure 4: Ultrastructural analyses of melanosomes of the retinal pigment epithelium (RPE) and choroid in single and multiple HPS AP-3/BLOC mutants. The interface between the RPE (above) and the choroid (below) is indicated in each case by a hyphenated partial line at left. Scale bar = 2 μm. Melanosomes of the BLOC-2⁻, 3⁻, AP-3⁻ triple mutant and the BLOC-1⁻, 2⁻, 3⁻, AP-3⁻ quadruple mutant were not analyzed due to the lack of sufficient numbers of mutants.

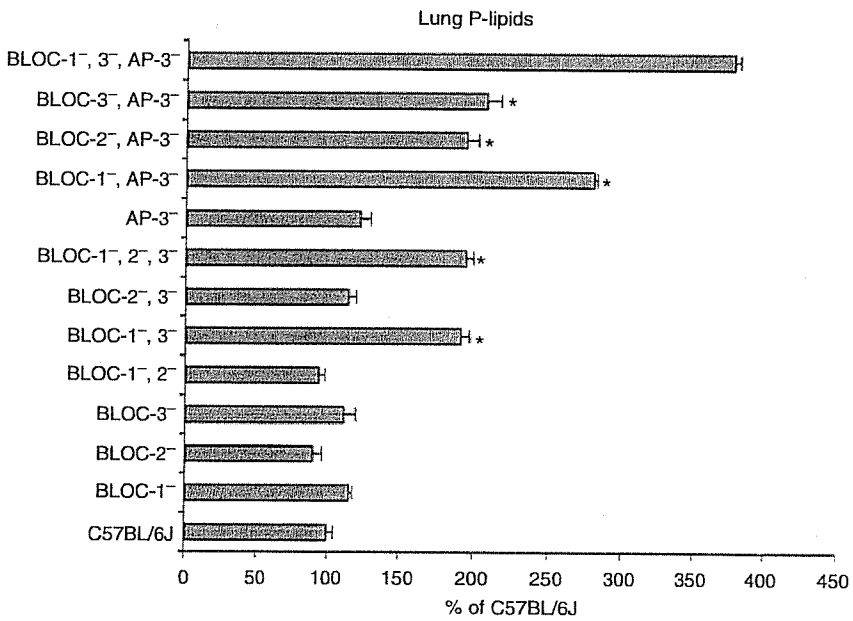

Figure 5: Phospholipid levels of multiple HPS mutants. Total lung phospholipid was measured in the lungs of multiple mutants by the Fiske–SubbaRow reagent and expressed relative to lung p-lipid concentrations of C57BL/6J. $n = 5$, *$p < 0.001$.

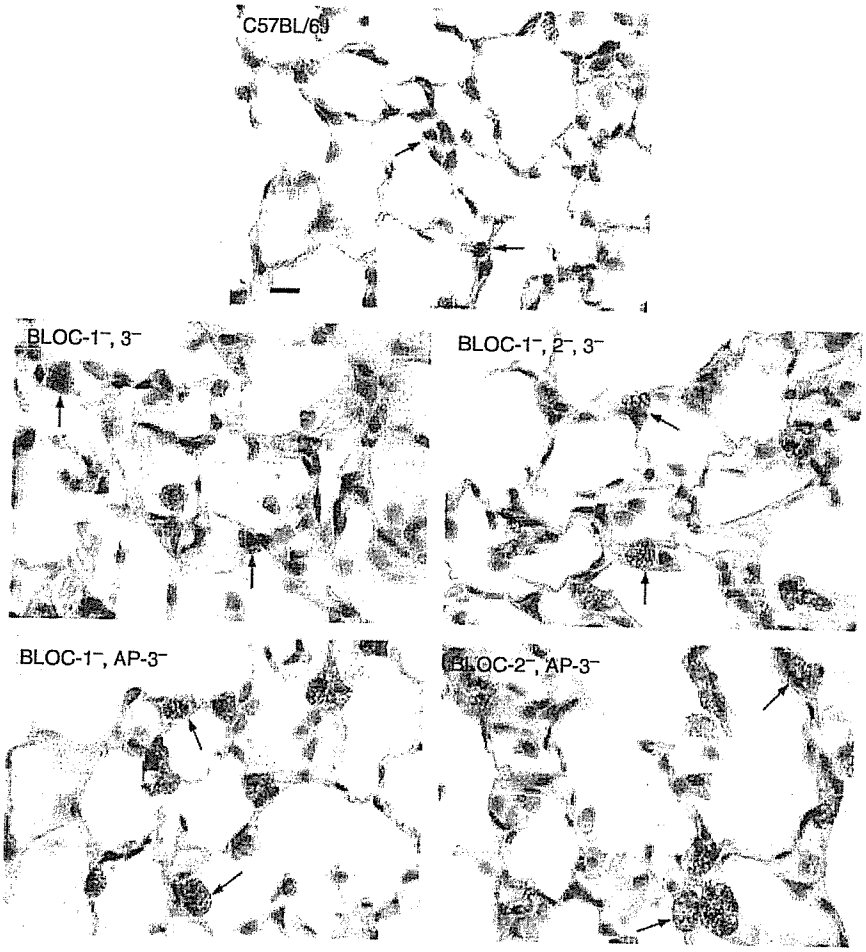

Figure 6: Enlarged lamellar bodies in lung type II cells of multiple HPS mutants. Antibody to surfactant protein B was used to detect lamellar bodies (arrows) in lungs of type II cells. Lung sections of the single mutants BLOC-1⁻, BLOC-2⁻, BLOC-3⁻ and AP-3⁻ single mutants (not shown) revealed lamellar bodies similar or slightly enlarged in size to those of C57BL/6J. Scale bar = 10 μm.

observed in the double mutant BLOC-2⁻, AP-3⁻ where lysosomal enzyme secretion is much less than either single mutant.

Discussion

In classical epistasis analyses, the phenotypes of single and corresponding double mutants are compared in the same background strain (15,27). By integrating the epistatic interactions between several pairs of genes, genetic networks outlining the details of biological processes and, in some cases, the order of function of genes in a pathway can be inferred. An advantage of the epistasis approach to dissecting the number of pathways involved in producing a given phenotype is that it is not necessary to know all the genes in all the pathways. We have utilized this approach to delineate interactions of the HPS BLOC and AP-3 protein complexes and the genes which encode them in the biosynthesis and function of LROs. These studies have also allowed us to evaluate the roles of HPS genes in *in vivo* viability, robustness and reproductive ability.

The interpretation of the phenotypes of the multiple mutants studied here is simplified by the fact that all mutants are maintained on a common C57BL/6J inbred strain background. The lone exception is a 50% contribution of genes from the closely related C57BL/10J background in the case of the BLOC-2⁻, 3⁻ double mutant. Thus there is minimal or no contribution of differing background genes in the multiple mutants to confound interpretations. Also, all are null mutations (3). A possible exception is that small residual function may occur in the pearl AP-3⁻ mutant (28). However, this is controversial as no expression of the beta3A subunit of the AP-3 complex was detectable by Northern blotting of tissues of the pearl allele utilized here (29). Further accentuating the null natures of these mutations are the well-documented destabilizations of other subunits of the particular BLOC or AP-3 complex affected by the mutation (30–32). For all these reasons we feel it is highly likely that the multiple mutants are true functional nulls for their respective complexes. Nevertheless, we have described these multiple mutants as 'deficient' in the various BLOC complexes and the AP-3 complex because we cannot rule out the unlikely possibility that the small residual levels of subunits of the affected